

Streamlined Empirical Bayes Fitting of Linear Mixed Models in Mobile Health

BY MARIANNE MENICTAS¹, SABINA TOMKINS² AND SUSAN A. MURPHY¹

Harvard University¹ Stanford University²

28 March, 2020

Abstract

To effect behavior change a successful algorithm must make high-quality decisions in real-time. For example, a mobile health (mHealth) application designed to increase physical activity must make contextually relevant suggestions to motivate users. While machine learning offers solutions for certain stylized settings, such as when batch data can be processed offline, there is a dearth of approaches which can deliver high-quality solutions under the specific constraints of mHealth. We propose an algorithm which provides users with contextualized *and* personalized physical activity suggestions. This algorithm is able to overcome a challenge critical to mHealth that complex models be trained efficiently. We propose a tractable streamlined empirical Bayes procedure which fits linear mixed effects models in large-data settings. Our procedure takes advantage of sparsity introduced by hierarchical random effects to efficiently learn the posterior distribution of a linear mixed effects model. A key contribution of this work is that we provide explicit updates in order to learn both fixed effects, random effects and hyper-parameter values. We demonstrate the success of this approach in a mobile health (mHealth) reinforcement learning application, a domain in which fast computations are crucial for real time interventions. Not only is our approach computationally efficient, it is also easily implemented with closed form matrix algebraic updates and we show improvements over state of the art approaches both in speed and accuracy of up to 99% and 56% respectively.

Keywords: empirical Bayes; Mixed models; Thompson sampling; mobile health; reinforcement learning.

1 Introduction

This work is motivated by a mobile health study in which an online Thompson Sampling contextual bandit algorithm is used to personalize the delivery of physical activity suggestions [1]. These suggestions are intended to increase near time physical activity. The personalization occurs via two routes, first the user’s current context is used to decide whether to deliver a suggestion and second, random effects, as described in Section 2.1, are used to learn user and time specific parameters that encode the influence of each of the contextual variables in this decision. The user and time specific parameters are modeled in the reward function (the mean of the reward conditional on context and action). To learn these parameters, information is pooled across both users and time in a dynamic manner, combining Thompson sampling with a Bayesian random effects model for the reward function. In contrast to fully Bayesian methods, empirical Bayes estimates the value of hyper-parameters as a function of observed data.

The contributions of this paper are as follows

- We develop a Thompson sampling algorithm coupled with explicit streamlined empirical Bayes updates for fitting linear mixed effects models. To estimate hyper-parameters and compute the estimated posterior distribution, our algorithm com-

puts closed form updates which are within the class of two-level sparse least squares problems introduced by [2].

- This work provides an efficient empirical Bayes algorithm in which the amount of storage and computing at each iteration is $\mathcal{O}(m_1 m_2^3)$, where m_1 is the larger dimension of the two grouping mechanisms considered. For example, m_1 may represent the number of users and m_2 the time points or vice-versa.
- Our approach reduces the running time over other state-of-art methods, and critically, does not require advanced hardware.

These contributions make our approach practical for online mHealth settings, in which incremental learning algorithm updates are required (e.g., at nightly increments), where swift computations are necessary for subsequent *online* policy adaptation. This facilitates incremental, accurate tuning of the variance hyper-parameters in a Thompson-Sampling contextual bandit algorithm.

In section 2.1 we describe the problem setting and review Thompson-Sampling with the use of a Bayesian mixed effects model for the reward [1]. Section 2.2 describes a natural parametric empirical Bayes approach to hyperparameter tuning and Section 2.3 presents our streamlined alternative. A performance assessment and comparison is shown in Section 3.

2 Methods

2.1 Problem Setting

At each time, t , on each user, i , a vector of context variables, \mathbf{X}_{it} , is observed. An action, A_{it} , is then selected. Here we consider K actions, where $K \in \mathbb{N}$. Subsequently a real-valued reward, Y_{it} is observed. This continues for $t = 1, \dots, T$ times and on $i = 1, \dots, m$ users. We assume that the reward at time t is generated with a person and time specific mean,

$$E[Y_{it} | \mathbf{X}_{it}, A_{it}] = \mathbf{Z}_{it} \boldsymbol{\beta} + \mathbf{Z}_{it}^u \mathbf{u}_i + \mathbf{Z}_{it}^v \mathbf{v}_t$$

where $\mathbf{Z}_{it} = f(\mathbf{X}_{it}, A_{it})$, $\mathbf{Z}_{it}^u = f^u(\mathbf{X}_{it}, A_{it})$ and $\mathbf{Z}_{it}^v = f^v(\mathbf{X}_{it}, A_{it})$ are known features of the context \mathbf{X}_{it} and action A_{it} . $(\boldsymbol{\beta}, \mathbf{u}_i, \mathbf{v}_i)$ are unknown parameters; in particular \mathbf{u}_i is the vector of i th user parameters and \mathbf{v}_t is the vector of time t parameters. Time t corresponds to “time-since-under-treatment” for a user. User-specific parameters, \mathbf{u}_i , capture unobserved user variables that influence the reward at all times t ; in mobile health unobserved user variables may include level of social support for activity, pre-existing problems or preferences that make activity difficult. The time-specific parameters, \mathbf{v}_t capture unobserved “time-since-under-treatment” variables that influence the reward for all users. In mobile health unobserved “time-since-under-treatment” variables might include treatment fatigue, decreasing motivation, etc.

The Thompson Sampling algorithm in [1] uses the following Bayesian mixed effects model for the reward Y_{it} :

$$Y_{it} | \boldsymbol{\beta}, \mathbf{u}_i, \mathbf{v}_t, \sigma_\varepsilon^2 \stackrel{\text{ind.}}{\sim} N(\mathbf{Z}_{it} \boldsymbol{\beta} + \mathbf{Z}_{it}^u \mathbf{u}_i + \mathbf{Z}_{it}^v \mathbf{v}_t, \sigma_\varepsilon^2). \quad (1)$$

The algorithm is designed with independent Gaussian priors on the unknown parameters:

$$\begin{aligned} \boldsymbol{\beta} &\sim N(\boldsymbol{\mu}_\beta, \boldsymbol{\Sigma}_\beta), & \mathbf{u}_i | \boldsymbol{\Sigma}^u &\stackrel{\text{ind.}}{\sim} N(\mathbf{0}, \boldsymbol{\Sigma}^u), & 1 \leq i \leq m, \\ \mathbf{v}_\tau | \boldsymbol{\Sigma}^v &\stackrel{\text{ind.}}{\sim} N(\mathbf{0}, \boldsymbol{\Sigma}^v), & 1 \leq \tau \leq t. \end{aligned} \quad (2)$$

The \mathbf{u}_i and \mathbf{v}_τ are called random effects in the statistical literature and the model in (1) and (2) is often referred to as a linear mixed effects model [3] or a linear mixed model with

crossed random effects (e.g., [4, 5]). At each time, t , Thompson Sampling is used to select the action, A_{it} , based on the context \mathbf{X}_{it} . That is, we compute the posterior distribution for $\boldsymbol{\theta}_{it}$ where

$$\boldsymbol{\theta}_{it} = [\boldsymbol{\beta} \ \mathbf{u}_i \ \mathbf{v}_t]^T,$$

and for context $\mathbf{X}_{it} = \mathbf{x}$, select treatment $A_{it} = k$ with posterior probability

$$\Pr_{\boldsymbol{\theta}_{it} \sim N(\boldsymbol{\mu}_{p(\boldsymbol{\theta}_{it})}, \boldsymbol{\Sigma}_{p(\boldsymbol{\theta}_{it})})} \left(E[Y_{it} | \mathbf{X}_{it} = \mathbf{x}, A_{it} = k] = \max_{a=1, \dots, K} \left\{ E[Y_{it} | \mathbf{X}_{it} = \mathbf{x}, A_{it} = a] \right\} \right) \quad (3)$$

where $(\boldsymbol{\mu}_{\boldsymbol{\theta}_{it}}, \boldsymbol{\Sigma}_{\boldsymbol{\theta}_{it}})$ are the posterior mean and variance covariance matrix given in the sub-blocks of (7).

2.1.1 Bayesian Mixed Effects Model Components

We define the following data matrices

$$\begin{aligned} \mathbf{Y} &\equiv [\mathbf{Y}_1 \ \dots \ \mathbf{Y}_m]^\top, \quad \mathbf{Y}_i \equiv [Y_{i1} \ \dots \ Y_{it}]^\top, \quad \mathbf{Z} \equiv [\mathbf{Z}_1 \ \dots \ \mathbf{Z}_m]^\top, \quad \mathbf{Z}_i \equiv [\mathbf{Z}_{i1} \ \dots \ \mathbf{Z}_{it}]^\top, \\ \mathbf{Z}_i^u &\equiv [\mathbf{Z}_{i1}^u \ \dots \ \mathbf{Z}_{it}^u]^\top, \quad \mathbf{Z}_i^v \equiv \begin{bmatrix} \mathbf{Z}_{i1}^v & \dots & \mathbf{0} \\ \vdots & \ddots & \vdots \\ \mathbf{0} & \dots & \mathbf{Z}_{it}^v \end{bmatrix}, \quad \mathbf{Z}^{uv} \equiv \begin{bmatrix} \mathbf{Z}_1^u & \dots & \mathbf{0} & \mathbf{Z}_1^v \\ \vdots & \ddots & \vdots & \vdots \\ \mathbf{0} & \dots & \mathbf{Z}_m^u & \mathbf{Z}_m^v \end{bmatrix}, \end{aligned}$$

and the following parameter vectors

$$\boldsymbol{\beta} \equiv [\beta_0 \ \dots \ \beta_{p-1}]^\top, \quad \mathbf{u} \equiv [\mathbf{u}_1 \ \dots \ \mathbf{u}_m]^\top, \quad \mathbf{v} \equiv [\mathbf{v}_1 \ \dots \ \mathbf{v}_t]^\top,$$

where, as before, $\mathbf{Z}_{it}^u = f^u(\mathbf{X}_{it}, A_{it})$ and $\mathbf{Z}_{it}^v = f^v(\mathbf{X}_{it}, A_{it})$ represent the known features of the context \mathbf{X}_{it} and action A_{it} . The dimensions of matrices, for $1 \leq i \leq m$ and $1 \leq \tau \leq t$, are

$$\begin{aligned} \mathbf{Z}_{i\tau} &\text{ is } 1 \times p, \quad \boldsymbol{\beta} \text{ is } p \times 1, \quad \mathbf{Z}_{i\tau}^u \text{ is } 1 \times q_u, \quad \mathbf{Z}_{i\tau}^v \text{ is } 1 \times q_v, \quad \mathbf{u}_i \text{ is } q_u \times 1, \\ \mathbf{v}_\tau &\text{ is } q_v \times 1, \quad \boldsymbol{\Sigma}_u \text{ is } q_u \times q_u \text{ and } \boldsymbol{\Sigma}_v \text{ is } q_v \times q_v. \end{aligned} \quad (4)$$

2.1.2 Posterior Updates

The posterior distribution $\boldsymbol{\theta}_{it}$ for the immediate treatment effect for user i at time t is updated and then used to assign treatment in the subsequent time point, $t + 1$. Here, we show the form of the full posterior for $[\boldsymbol{\beta} \ \mathbf{u} \ \mathbf{v}]^\top$. Define

$$\begin{aligned} \mathbf{C} &\equiv [\mathbf{Z} \ \mathbf{Z}^{uv}], \quad \mathbf{D} \equiv \begin{bmatrix} \boldsymbol{\Sigma}_\beta^{-1} & \mathbf{0} & \mathbf{0} \\ \mathbf{0} & \mathbf{I}_m \otimes \hat{\boldsymbol{\Sigma}}_u^{-1} & \mathbf{0} \\ \mathbf{0} & \mathbf{0} & \mathbf{I}_t \otimes \hat{\boldsymbol{\Sigma}}_v^{-1} \end{bmatrix}, \\ \mathbf{R} &\equiv \hat{\sigma}_\varepsilon^2 \mathbf{I}, \quad \text{and} \quad \mathbf{o} \equiv \begin{bmatrix} \boldsymbol{\Sigma}_\beta^{-1} \boldsymbol{\mu}_\beta \\ \mathbf{0} \end{bmatrix}. \end{aligned}$$

The estimated posterior distribution for the fixed and random reward effects vector $\boldsymbol{\theta}$ is

$$\boldsymbol{\theta} | \hat{\boldsymbol{\Sigma}} \sim N\left(\boldsymbol{\mu}_{p(\boldsymbol{\theta})}, \boldsymbol{\Sigma}_{p(\boldsymbol{\theta})}\right), \quad (5)$$

where

$$\hat{\boldsymbol{\Sigma}} \equiv (\hat{\sigma}_\varepsilon^2, \hat{\boldsymbol{\Sigma}}_u, \hat{\boldsymbol{\Sigma}}_v), \quad (6)$$

$$\boldsymbol{\Sigma}_{p(\boldsymbol{\theta})} = (\mathbf{C}^\top \mathbf{R}^{-1} \mathbf{C} + \mathbf{D})^{-1}, \quad \text{and} \quad \boldsymbol{\mu}_{p(\boldsymbol{\theta})} = (\mathbf{C}^\top \mathbf{R}^{-1} \mathbf{C} + \mathbf{D})^{-1} (\mathbf{C}^\top \mathbf{R}^{-1} \mathbf{y} + \mathbf{o}). \quad (7)$$

The focus of this work is to enable fast incremental estimation of the variance components $\boldsymbol{\Sigma} \equiv (\sigma_\varepsilon^2, \boldsymbol{\Sigma}_u, \boldsymbol{\Sigma}_v)$. We describe a natural, but computationally challenging approach for estimating these variances in Section 2.2 and our streamlined alternative approach in Section 2.3.

2.2 Parametric Empirical Bayes

At each time, t , the empirical Bayes [6, 7] procedure maximizes the marginal likelihood based on all user data up to and including data at time t with respect to Σ . The marginal likelihood of \mathbf{Y} is

$$\mathbf{Y} | \Sigma \sim N(\mathbf{0}, \mathbf{C} \mathbf{D} \mathbf{C}^\top + \sigma_\varepsilon^2 \mathbf{I}),$$

and has the following form

$$p(\mathbf{Y} | \Sigma) = (2\pi)^{-\frac{1}{2}mt} |\mathbf{C} \mathbf{D} \mathbf{C}^\top + \sigma_\varepsilon^2 \mathbf{I}|^{-\frac{1}{2}} \exp \left\{ -\frac{1}{2} \mathbf{Y}^\top (\mathbf{C} \mathbf{D} \mathbf{C}^\top + \sigma_\varepsilon^2 \mathbf{I})^{-1} \mathbf{Y} \right\}.$$

The maximization is commonly done via the Expectation Maximisation (EM) algorithm [8].

2.2.1 EM Method

The expected complete data log likelihood is given by

$$L(\Sigma) = E [\log p(\mathbf{Y} | \boldsymbol{\theta}, \Sigma) + \log p(\boldsymbol{\theta} | \Sigma)]$$

where the expectation is over the distribution of $\boldsymbol{\theta} = [\boldsymbol{\beta} \ \mathbf{u} \ \mathbf{v}]^\top$ given in (2). The M-step yields the following closed form $(\ell + 1)$ iteration estimates for the variance components in $\hat{\Sigma}^{(\ell+1)}$:

$$\begin{aligned} (\hat{\sigma}_\varepsilon^2)^{(\ell+1)} &= \sum_{i=1}^m \sum_{\tau=1}^t \left\{ \|Y_{i\tau} - \mathbf{Z}_{i\tau} \boldsymbol{\mu}_{p(\boldsymbol{\beta})} - \mathbf{Z}_{i\tau}^u \boldsymbol{\mu}_{p(\mathbf{u}_i)} - \mathbf{Z}_{i\tau}^v \boldsymbol{\mu}_{p(\mathbf{v}_\tau)}\|^2 + \text{tr} \left(\mathbf{Z}_{i\tau}^\top \mathbf{Z}_{i\tau} \boldsymbol{\Sigma}_{p(\boldsymbol{\beta})} \right) \right. \\ &\quad + \text{tr} \left(\mathbf{Z}_{i\tau}^{u\top} \mathbf{Z}_{i\tau}^u \boldsymbol{\Sigma}_{p(\mathbf{u}_i)} \right) + \text{tr} \left(\mathbf{Z}_{i\tau}^{v\top} \mathbf{Z}_{i\tau}^v \boldsymbol{\Sigma}_{p(\mathbf{v}_\tau)} \right) \\ &\quad + \text{tr} \left(\mathbf{Z}_{i\tau}^\top \mathbf{Z}_{i\tau}^u \mathbf{Cov}_{p(\boldsymbol{\beta}, \mathbf{u}_i)} \right) + \text{tr} \left(\mathbf{Z}_{i\tau}^\top \mathbf{Z}_{i\tau}^v \mathbf{Cov}_{p(\boldsymbol{\beta}, \mathbf{v}_\tau)} \right) \\ &\quad \left. + \text{tr} \left(\mathbf{Z}_{i\tau}^{u\top} \mathbf{Z}_{i\tau}^v \mathbf{Cov}_{p(\mathbf{u}_i, \mathbf{v}_\tau)} \right) \right\}, \\ \hat{\boldsymbol{\Sigma}}_{\mathbf{u}}^{(\ell+1)} &= \frac{1}{m} \sum_{i=1}^m \left\{ \boldsymbol{\mu}_{p(\mathbf{u}_i)} \boldsymbol{\mu}_{p(\mathbf{u}_i)}^\top + \boldsymbol{\Sigma}_{p(\mathbf{u}_i)} \right\}, \\ \hat{\boldsymbol{\Sigma}}_{\mathbf{v}}^{(\ell+1)} &= \frac{1}{t} \sum_{\tau=1}^t \left\{ \boldsymbol{\mu}_{p(\mathbf{v}_\tau)} \boldsymbol{\mu}_{p(\mathbf{v}_\tau)}^\top + \boldsymbol{\Sigma}_{p(\mathbf{v}_\tau)} \right\}. \end{aligned} \tag{8}$$

where the posterior mean reward components for the fixed and random effects

$$\boldsymbol{\mu}_{p(\boldsymbol{\beta})}, \boldsymbol{\mu}_{p(\mathbf{u}_i)}, 1 \leq i \leq m, \quad \boldsymbol{\mu}_{p(\mathbf{v}_\tau)}, 1 \leq \tau \leq t, \tag{9}$$

and the posterior variance-covariance reward components for the fixed and random effects

$$\begin{aligned} \boldsymbol{\Sigma}_{p(\boldsymbol{\beta})}, \boldsymbol{\Sigma}_{p(\mathbf{u}_i)}, \boldsymbol{\Sigma}_{p(\mathbf{v}_\tau)}, \quad \mathbf{Cov}_{p(\boldsymbol{\beta}, \mathbf{u}_i)}, \mathbf{Cov}_{p(\boldsymbol{\beta}, \mathbf{v}_\tau)}, \mathbf{Cov}_{p(\mathbf{u}_i, \mathbf{v}_\tau)}, \\ 1 \leq i \leq m, 1 \leq \tau \leq t, \end{aligned} \tag{10}$$

are computed in the E-step using equation (7). Note that (9) are the sub vectors in the posterior mean $\boldsymbol{\mu}_{p(\boldsymbol{\theta})}$ and (10) are sub-block entries in the posterior variance covariance matrix $\boldsymbol{\Sigma}_{p(\boldsymbol{\theta})}$. The naïve EM algorithm is given in Algorithm 1. The challenge in Algorithm 1 is computation of the posterior mean vector $\boldsymbol{\mu}_{p(\boldsymbol{\theta})}$ and posterior variance-covariance matrix $\boldsymbol{\Sigma}_{p(\boldsymbol{\theta})}$ at each iteration. We discuss the details of these challenges in Section 2.2.2.

Algorithm 1 *Naïve EM Algorithm for empirical Bayes estimates of the variance components in the Bayesian mixed effects model as given in (1) and (2).*

Initialize: $\hat{\Sigma}^{(0)}$

Set $\ell = 0$

repeat

E-step: Compute $\mu_{p(\theta)}$ and $\Sigma_{p(\theta)}$ via equation (7) to obtain necessary mean and variance-covariance components needed for the M-step.

M-step: Compute variance components in $\hat{\Sigma}^{(\ell+1)}$ via equation (8).

$\ell \leftarrow \ell + 1$

until log-likelihood converges

2.2.2 Computational Challenges

At each iteration in Algorithm 1, computation of $p(\theta)$ requires solving the sparse matrix linear system

$$\mathbf{C}^\top \mathbf{R}^{-1} \mathbf{C} + \mathbf{D} = \mathbf{C}^\top \mathbf{R}^{-1} \mathbf{Y} + \mathbf{o} \quad (11)$$

where the LHS of (11) has sparse structure imposed by the random effects as exemplified in Figure 1. This matrix has dimension

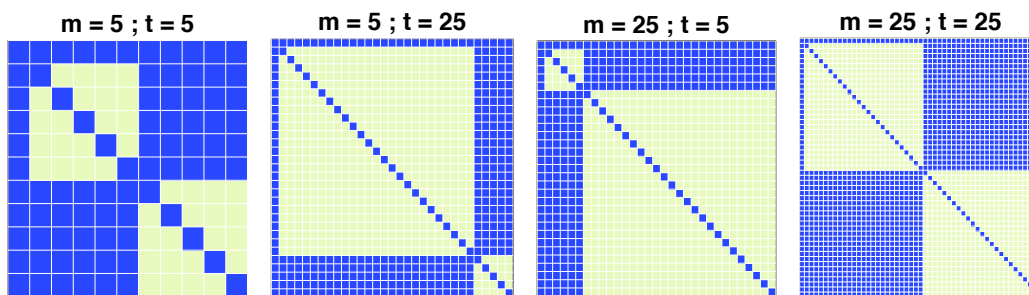


Figure 1: *Sparsity present in $\mathbf{C}^\top \mathbf{R}^{-1} \mathbf{C} + \mathbf{D}$ under the Bayesian mixed effects model as represented in (1) and (2). Here, $p = q_u = q_v = 1$. Non-zero 1×1 entries are represented by a blue square and zero 1×1 entries are represented by a light-yellow square.*

$$(p + mq_u + tq_v) \times (p + mq_u + tq_v).$$

It is often the case that the number of fixed effects parameters p , the number of random effects parameters per user q_u and the number of random effects parameters per time q_v are of moderate size. Consequently, it is well known that naïve computation of $p(\theta)$ is $\mathcal{O}((m+t)^3)$, that is, cubic dependence on the number of random effects group sizes m and t .

To address this computational problem, we employ the fact that in this setting the matrix requiring inversion is sufficiently block-diagonal that its sparsity can be exploited. In addition, the closed form updates of the variance components in (8) require computation of only the sub-blocks of $\Sigma_{p(\theta)}$ that correspond to the non-zero sub-blocks of $\mathbf{C}^\top \mathbf{R}^{-1} \mathbf{C} + \mathbf{D}$ (as illustrated in Figure 1) and not the entire matrix.

2.3 Streamlined Empirical Bayes

Streamlined updating of $\mu_{p(\theta)}$ and each of the sub-blocks of $\Sigma_{p(\theta)}$ required for the E-step in Algorithm 1 can be embedded within the class of two-level sparse matrix problems as defined in [9] and is encapsulated in Result 1. Result 1 is analogous and mathematically identical to Result 2 in [10]. The difference being that the authors in [10] do not apply

their methodologies to the mobile health setting and use full variational Bayesian inference for fitting as opposed to our use of empirical Bayes.

Result 1 (*Analogous and mathematically identical to Result 2 in [10]*). *The posterior updates under the Bayesian mixed effects model as given in (1) and (2) for $\boldsymbol{\mu}_{p(\boldsymbol{\theta})}$ and each of the sub-blocks of $\boldsymbol{\Sigma}_{p(\boldsymbol{\theta})}$ are expressible as a two-level sparse matrix least squares problem of the form $\|\mathbf{b} - \mathbf{B} \boldsymbol{\mu}_{p(\boldsymbol{\theta})}\|^2$ where \mathbf{b} and the non-zero sub-blocks of \mathbf{B} , according to the notation in the appendix, are, for $1 \leq i \leq m$,*

$$\mathbf{b}_i \equiv \begin{bmatrix} \sigma_\varepsilon^{-1} \mathbf{Y}_i \\ m^{-\frac{1}{2}} \boldsymbol{\Sigma}_\beta^{-\frac{1}{2}} \boldsymbol{\mu}_\beta \\ \mathbf{0} \\ \mathbf{0} \end{bmatrix}, \quad \dot{\mathbf{B}}_i \equiv \begin{bmatrix} \sigma_\varepsilon^{-1} \mathbf{Z}_i^u \\ \mathbf{O} \\ \mathbf{O} \\ \boldsymbol{\Sigma}_u^{-\frac{1}{2}} \end{bmatrix}, \quad \mathbf{B}_i \equiv \begin{bmatrix} \sigma_\varepsilon^{-1} \mathbf{X}_i & \sigma_\varepsilon^{-1} \mathbf{Z}_i^v \\ m^{-\frac{1}{2}} \boldsymbol{\Sigma}_\beta^{-\frac{1}{2}} & \mathbf{O} \\ \mathbf{O} & m^{-\frac{1}{2}} \left(\mathbf{I}_t \otimes \boldsymbol{\Sigma}_v^{-\frac{1}{2}} \right) \\ \mathbf{O} & \mathbf{O} \end{bmatrix},$$

with each of these matrices having $\tilde{n} = t + p + tq_v + q_u$ rows. The solutions are

$$\boldsymbol{\mu}_{p(\beta)} = \text{first } p \text{ rows of } \mathbf{x}_1, \quad \boldsymbol{\Sigma}_{p(\beta)} = \text{top left } p \times p \text{ sub-block of } \mathbf{A}^{11},$$

$$\text{stack}_{1 \leq i \leq m} \left(\boldsymbol{\mu}_{p(u_i)} \right) = \text{subsequent } q_u \times 1 \text{ entries of } \mathbf{x}_1 \text{ following } \boldsymbol{\mu}_{p(\beta)},$$

$$\boldsymbol{\Sigma}_{p(u_i)} = \text{subsequent } q_u \times q_u \text{ diagonal sub-blocks of } \mathbf{A}^{11} \text{ following } \boldsymbol{\Sigma}_{p(\beta)},$$

$$\mathbf{Cov}_{p(\beta, u_i)} = \text{subsequent } p \times q' \text{ sub-blocks of } \mathbf{A}^{11} \text{ to the right of } \boldsymbol{\Sigma}_{p(\beta)}, \quad 1 \leq i \leq m,$$

$$\boldsymbol{\mu}_{p(v_\tau)} = \mathbf{x}_{2,\tau}, \quad \boldsymbol{\Sigma}_{p(v_\tau)} = \mathbf{A}^{22,\tau}, \quad \mathbf{Cov}_{p(\beta, v_\tau)} = \text{first } p \text{ rows of } \mathbf{A}^{12,\tau}$$

and

$$\text{stack}_{1 \leq i \leq m} \left(\mathbf{Cov}_{p(u_i, v_\tau)} \right) = \text{remaining } q_u \text{ rows of } \mathbf{A}^{12,\tau},$$

$1 \leq \tau \leq t$, where the \mathbf{x}_1 , $\mathbf{x}_{2,\tau}$, \mathbf{A}^{11} , $\mathbf{A}^{22,\tau}$ and $\mathbf{A}^{12,\tau}$ notation is given in the appendix.

The streamlined equivalent of Algorithm 1 is given in Algorithm 2. Algorithm 2 makes use of the SOLVETWOLEVELSPARSELEASTSQUARES algorithm which was first presented in [9] but also provided in the appendix of this article. The computing time and storage for

Algorithm 2 *Streamlined EM algorithm for empirical Bayes estimates of the variance components in the Bayesian mixed effects model as given in (1) and (2).*

Initialize: $\hat{\boldsymbol{\Sigma}}^{(0)}$

Set $\ell = 0$

repeat

E-step: Compute components of $\boldsymbol{\mu}_{p(\boldsymbol{\theta})}$ and sub-blocks of $\boldsymbol{\Sigma}_{p(\boldsymbol{\theta})}$:

$\mathcal{S} \leftarrow \text{SOLVETWOLEVELSPARSELEASTSQUARES}(\{(\mathbf{b}_i, \mathbf{B}_i, \dot{\mathbf{B}}_i) : 1 \leq i \leq m\})$

where

\mathcal{S} returns \mathbf{x}_1 , \mathbf{A}^{11} , $\mathbf{x}_{2,i}$, $\mathbf{A}^{22,i}$ and $\mathbf{A}^{12,i}$, $1 \leq i \leq m$.

M-step: Compute variance components in $\hat{\boldsymbol{\Sigma}}^{(\ell+1)}$ via equation (8).

$\ell \leftarrow \ell + 1$

until log-likelihood converges

the streamlined updating of $\boldsymbol{\mu}_{p(\boldsymbol{\theta})}$ and each of the sub-blocks of $\boldsymbol{\Sigma}_{p(\boldsymbol{\theta})}$ required for the E-step in Algorithm 2 becomes $\mathcal{O}(mt^3)$. For moderate sized t , this reduces to $\mathcal{O}(m)$. If both m and t are large, one may resort to coupling the streamlining present in this article

with an approximation of the posterior so as to further reduce computation time and storage. However, care needs to be taken with the choice of approximation so as to incur as little degradation in accuracy as possible. As explained in Section 3.1 of [11], mean field variational Bayes approximations tend to be very accurate for Gaussian response models. However, such high accuracy does not manifest in general. Ignoring important posterior dependencies via mean field restrictions often lead to credible intervals being too small (e.g. [12]).

3 Performance Assessment and Comparison

In order to evaluate the speed achieved by our streamlined empirical Bayes algorithm, we compare the timing and accuracy of our method against state of the art software, `GPYtorch` [13], which is a highly efficient implementation of Gaussian Process Regression modeling, with GPU acceleration. Note that the Gaussian linear mixed effects model as given in (1) and (2) is equivalent to a Gaussian Process regression model with a structured kernel matrix induced by the use of random effects. For ease of notation, in the following, we use `sEB` to refer to the streamlined empirical Bayes algorithm, `GPYT-CPU` to refer to empirical Bayes fitting using `GPYtorch` with CPU and `GPYT-GPU` to refer to empirical Bayes fitting using `GPYtorch` with GPU. The `sEB` and `GPYT-CPU` computations were conducted using an Intel Xeon CPU E5-2683. The `GPYT-GPU` computations were conducted using an Nvidia Tesla V100-PCIE-32GB.

3.1 Batch Speed Assessment

We obtained timing results for simulated batch data according to versions of the Bayesian mixed effects model as given in (1) and (2) and for which both the fixed effects and random effects had dimension two, corresponding to random intercepts and slopes for a single continuous predictor which was generated from the Uniform distribution on the unit interval. The true parameter values were set to

$$\beta_{\text{true}} = \begin{bmatrix} 0.58 \\ 1.98 \end{bmatrix}, \quad \Sigma_{\text{true}}^u = \begin{bmatrix} 0.32 & 0.09 \\ 0.09 & 0.42 \end{bmatrix}, \quad \Sigma_{\text{true}}^v = \begin{bmatrix} 0.30 & 0 \\ 0 & 0.25 \end{bmatrix}, \quad \text{and} \quad \sigma_{\varepsilon, \text{true}}^2 = 0.3,$$

and, during the studies, the t values were set to 30, and the number of datapoints specific to each user and time period, n , was set to 5. Four separate studies were run with differing values for the number of users $m \in \{10, 50, 100, 10000\}$. The total number of data points is then ntm , that is, datapoints $\in \{1500, 7500, 15000, 1500000\}$. We then simulated 50 replications of the data for each m and recorded the computational times for variance estimation from `GPYT-CPU`, `GPYT-GPU` and `sEB`. Algorithm 2 was implemented in `Fortran 77`. The EM iterations were stopped once the absolute difference between successive expected complete data log-likelihood values fell below 10^{-5} . The stopping criterion was the same for `gPyTorch` and additionally the maximum number of iterations was set to 15.

Table 1 shows the mean and standard deviation of elapsed computing times in seconds for estimation of the variance components using `sEB`, `GPYT-CPU` and `GPYT-GPU`. Figure 2 shows the absolute error values for each variance components estimated using `sEB`, `GPYT-CPU` and `GPYT-GPU` summarized as a boxplot.

3.2 Online Thompson Sampling Contextual Bandit mHealth Simulation Study

Next, we evaluate our approach in a simulated mHealth study designed to capture many of the real-world difficulties of mHealth clinical trials. Users in this simulated study are sent interventions multiple times each day according to Algorithm 3. Each intervention represents a message promoting healthy behavior.

Datapoints	sEB	GPyT-CPU	GPyT-GPU
1,500	0.7 (0.10)	5.8 (0.14)	1.5 (0.16)
7,500	1.7 (0.15)	163.8 (1.81)	1.3 (0.04)
15,000	2.8 (0.21)	736.2 (38.36)	5.2 (0.03)
1,500,000	322.1 (24.82)	NA (NA)	NA (NA)

Table 1: Mean (standard deviation) of elapsed computing times in seconds for estimation of the variance components in the Bayesian mixed effects model as represented in (1) and (2) using sEB via Algorithm 2, GPyT-CPU and GPyT-GPU for comparison.

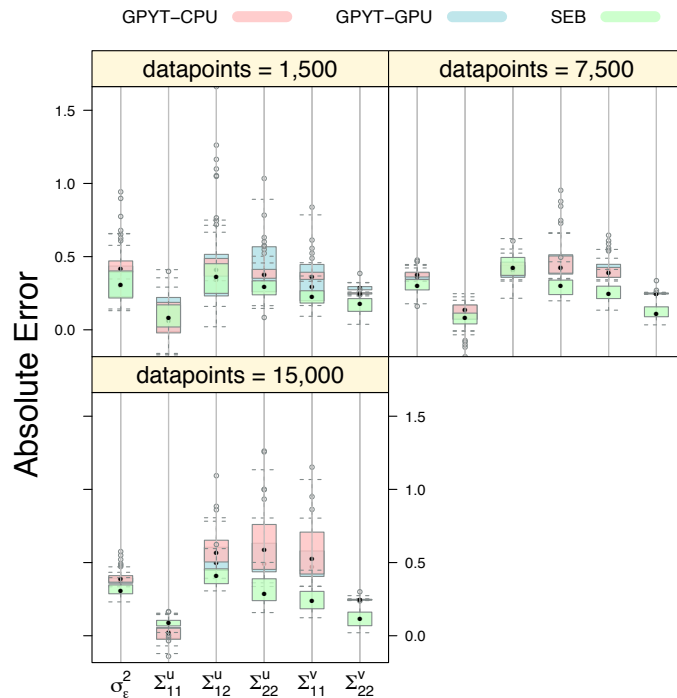


Figure 2: Summary of the simulation study in Section 3.1 under the Bayesian mixed effects model as represented in (1) and (2) where the absolute error values for each variance component estimated using one of three empirical Bayes methods summarized as a boxplot.

In this setting there are 32 users and each user is in the study for 10 weeks. Users join the study in a staggered fashion, such that each week new users might be joining or leaving the study. Each day in the study users can receive up to 5 mHealth interventions.

The Bayesian mixed effects model as represented in (1) and (2) offers several advantages in this setting. In mHealth not only can users differ in the context that they experience, but in their response to treatment under the same context. The user level random effects \mathbf{u}_i allow learning of personalized policies for each user, overcoming the flaws of methods which treat individuals as the same. Additionally, there can be non-stationarity in how users respond to treatment, for example, they might be more responsive in the beginning of a study than in the end. By modeling time level random effects \mathbf{v}_t , each person’s policy can be sensitive to a dynamic environment, and is informed by how other users’ responsivity has been influenced by time.

We evaluate our approach in a setting which demands personalization within a dynamic environment. Users are modeled to be heterogenous in their response to treatment. Additionally, their responsivity declines with time.

In Figure 3 we show the ability of our streamlined algorithm to minimize regret where

Algorithm 3 *Thompson-Sampling algorithm with linear mixed effects model as given in (1) and (2) for the reward.*

Initialize: $\hat{\sigma}_\varepsilon^2, \hat{\Sigma}_u, \hat{\Sigma}_v$

for $t \in \{t_1, \dots, t_T\}$:

for $\tau = 1, \dots, t$:

 Receive context features $\mathbf{X}_{i\tau}$ for user i and time τ

 Obtain posterior $p(\boldsymbol{\theta}_{i\tau})$ using Result 1

 Calculate randomization probability π in (3)

 Sample treatment $A_{i\tau} \sim \text{Bern}(\pi)$

 Observe reward $Y_{i\tau}$

if $\tau = t$:

 Update hyper-parameters $\hat{\Sigma}$ with Algorithm 2

 Update posterior $p(\boldsymbol{\theta}_{it})$

real data is used to inform the simulation. We also compare our approach to GPyT-CPU and GPyT-GPU. For all users we show the average performance for their n th week in the study. For example, we first show the average regret across all users in their first week of the study, however this will not be the same calendar time week, as users join in a staggered manner. The average total time (standard deviation) for estimation of the variance components was 757.1 (76.48) using GPyT-CPU, 7.5 (0.27) using GPyT-GPU and 7.3 (0.16) using sEB.

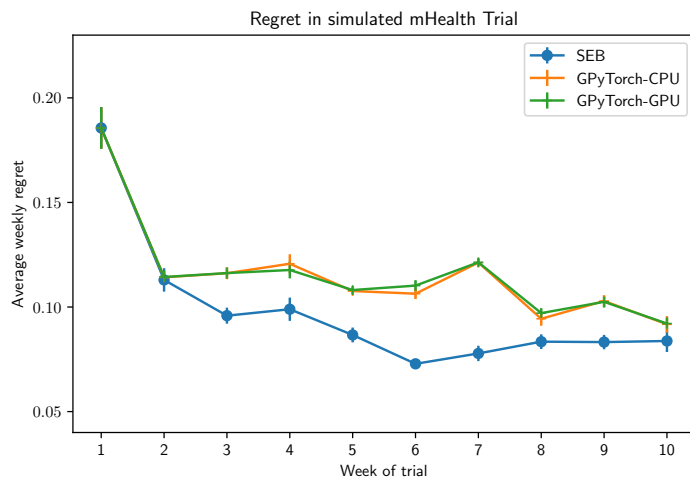


Figure 3: *Regret averaged across all users for each week in the simulated mHealth trial associated with approaches sEB, GPyT-CPU and GPyT-GPU.*

4 Related Work

The fundamental streamlined empirical Bayes Algorithm 2 makes use of linear system solutions and sub-block matrix inverses for two-level sparse matrix problems ([2]). Our result for streamlined posterior computation in Section 2.3 is analogous and mathematically identical to Result 2 in [10] who instead focus on streamlined mean field variational Bayes approximate inference for linear mixed models with crossed random effects. In the present article, we make use of a similar result for empirical Bayes posterior inference for use in the mobile health setting. Our empirical Bayes algorithm allows streamlined estimation of the variance components within an online Thompson sampling contextual bandit algorithm.

Other approaches include using mixed model software packages for high-performance statistical computation. For example: (i) **BLME** provides a posteriori estimation for linear and generalized linear mixed effects models in a Bayesian setting [14]; and (ii) **Stan** [15] provides full Bayesian statistical inference with MCMC sampling. Even though **BLME** offers streamlined algorithms for obtaining the predictions of fixed and random effects in linear mixed models, the sub-blocks of the covariance matrices of the posterior required for construction of the EM method in the streamlined empirical Bayes algorithm are not provided by such software. On the other hand, **Stan** does offer support for computation of these sub-blocks, but is well known to suffer computationally in large data settings.

As we point to in Section 3, the Gaussian linear mixed effects model used in the Thompson-Sampling algorithm is equivalent to a Gaussian Process regression model with a structured kernel matrix induced by the use of random effects. Gaussian process models have been used for multi-armed bandits ([16, 17, 18, 19, 20, 21, 22, 23]), and for contextual bandits ([24, 25]). To address the challenges posed by mHealth, [1] illustrate the benefits of using mixed effects Gaussian Process models in the context of reinforcement learning. Computational challenges in the Gaussian Process regression setting is a known and common problem which has led to contributions from the computer science and machine learning communities. For instance, to address challenges posed for Gaussian Process regression suffering from cubic complexity to data size, a variety of scalable GPs have been presented, including the approach we compare to earlier: **GPYtorch** [13]. A review on state-of-the-art scalable GPs involving two main categories: global approximations which distillate the entire data and local approximations which divide the data for subspace learning can be found in [26]. The sparsity imposed by the use of random effects, however, afford us accurate inference in the cases considered in this article, and thus do not suffer from the potential loss of accuracy that could result from the approximate methods, such as those discussed in [26].

5 Discussion

We compare three empirical Bayes approaches, **sEB**, **GPYT-CPU** and **GPYT-GPU** for use within a batch simulation setting and an online contextual bandit mHealth simulation study.

Within the batch simulation setting in Section 3.1, inspection of the computational running times in Table 1 shows that **sEB** achieves the lowest average running time across all simulations and data set sizes, compared to **GPYT-CPU** and **GPYT-GPU**. In the starkest case this results in a 98.96% reduction in running time. Even in the more modest comparison, **sEB** timing is similar to that of **GPYT-GPU** but doesn't require the sophisticated hardware that **GPYT-GPU** does. The improvement between **GPYT-CPU** and **GPYT-GPU** is impressive and **GPYT-GPU** is clearly designed to excel in a resource rich environment. However, in a clinical trial it is unclear if such an environment will be available. In contrast, **sEB** does not require advanced hardware to achieve state-of-the-art performance.

Our method makes use of computing only the necessary sub-blocks of the posterior variance-covariance matrix at each time step, as opposed to computation of the entire matrix. We were unable to template an equivalent streamlined computation within **GPYT-CPU** and **GPYT-GPU**. Consequently, we were unable to run **GPYT-CPU** and **GPYT-GPU** on the largest dataset as this involves constructing a matrix of dimension $(1.5 \times 10^6) \times (1.5 \times 10^6)$, even before the optimization procedure is called. Templating the variance-covariance matrix such that it did not require this matrix as input might have allowed us to run **GPYT-GPU** on the largest dataset. An advantage of our method is that it can efficiently exploit the structure inherent within the variance-covariance matrix to manage large datasets.

The median reduction in error from **GPYT-CPU** to **sEB** is 28.3% and from **GPYT-GPU** to **sEB** is 22.2%. From Figure 2, we see that **sEB** achieves lower absolute error on average than either **GPYT-CPU** or **GPYT-GPU**. The difference is more pronounced between **sEB** and **GPYT-GPU**. **sEB** achieves the lowest average absolute error, at the fastest rate, on the simplest machine.

References

- [1] Sabina Tomkins, Peng Liao, Serena Yeung, Predrag Klasnja, and Susan Murphy. Intelligent pooling in thompson sampling for rapid personalization in mobile health. 2019.
- [2] Tui H Nolan and Matt P Wand. Solutions to sparse multilevel matrix problems. *arXiv preprint arXiv:1903.03089*, 2019.
- [3] Nan M Laird, James H Ware, et al. Random-effects models for longitudinal data. *Biometrics*, 38(4):963–974, 1982.
- [4] R Harald Baayen, Douglas J Davidson, and Douglas M Bates. Mixed-effects modeling with crossed random effects for subjects and items. *Journal of memory and language*, 59(4):390–412, 2008.
- [5] Minjeong Jeon, Frank Rijmen, and Sophia Rabe-Hesketh. A variational maximization–maximization algorithm for generalized linear mixed models with crossed random effects. *psychometrika*, 82(3):693–716, 2017.
- [6] Carl N Morris. Parametric empirical bayes inference: theory and applications. *Journal of the American statistical Association*, 78(381):47–55, 1983.
- [7] George Casella. An introduction to empirical bayes data analysis. *The American Statistician*, 39(2):83–87, 1985.
- [8] Arthur P Dempster, Nan M Laird, and Donald B Rubin. Maximum likelihood from incomplete data via the em algorithm. *Journal of the Royal Statistical Society: Series B (Methodological)*, 39(1):1–22, 1977.
- [9] Tui H Nolan, Marianne Menictas, and Matt P Wand. Streamlined computing for variational inference with higher level random effects. *arXiv preprint arXiv:1903.06616*, 2019.
- [10] Marianne Menictas, Gioia Di Credico, and Matt P Wand. Streamlined variational inference for linear mixed models with crossed random effects. *arXiv preprint arXiv:1910.01799*, 2019.
- [11] Marianne Menictas and Matt P Wand. Variational inference for heteroscedastic semi-parametric regression. *Australian & New Zealand Journal of Statistics*, 57(1):119–138, 2015.
- [12] Bo Wang and DM Titterton. Inadequacy of interval estimates corresponding to variational bayesian approximations. In *AISTATS*. Citeseer, 2005.
- [13] Jacob Gardner, Geoff Pleiss, Kilian Q Weinberger, David Bindel, and Andrew G Wilson. Gpytorch: Blackbox matrix-matrix gaussian process inference with gpu acceleration. In *Advances in Neural Information Processing Systems*, 2018.
- [14] V Dorie. blme: Bayesian linear mixed-effects models. URL: <https://CRAN.R-project.org/package=blme> R package version, pages 1–0, 2015.
- [15] Bob Carpenter, Andrew Gelman, Matthew D Hoffman, Daniel Lee, Ben Goodrich, Michael Betancourt, Marcus Brubaker, Jiqiang Guo, Peter Li, and Allen Riddell. Stan: A probabilistic programming language. *Journal of statistical software*, 76(1), 2017.
- [16] Sayak Ray Chowdhury and Aditya Gopalan. On kernelized multi-armed bandits. In *Proceedings of the 34th International Conference on Machine Learning-Volume 70*, pages 844–853. JMLR. org, 2017.

- [17] Matthew D Hoffman, Eric Brochu, and Nando de Freitas. Portfolio allocation for bayesian optimization. In *UAI*, pages 327–336. Citeseer, 2011.
- [18] Sivaram Ambikasaran, Daniel Foreman-Mackey, Leslie Greengard, David W Hogg, and Michael O’Neil. Fast direct methods for gaussian processes. *IEEE transactions on pattern analysis and machine intelligence*, 38(2):252–265, 2015.
- [19] Niranjan Srinivas, Andreas Krause, Sham M Kakade, and Matthias Seeger. Gaussian process optimization in the bandit setting: No regret and experimental design. *arXiv preprint arXiv:0912.3995*, 2009.
- [20] Thomas Desautels, Andreas Krause, and Joel W Burdick. Parallelizing exploration-exploitation tradeoffs in gaussian process bandit optimization. *The Journal of Machine Learning Research*, 15(1):3873–3923, 2014.
- [21] Zi Wang, Bolei Zhou, and Stefanie Jegelka. Optimization as estimation with gaussian processes in bandit settings. In *Artificial Intelligence and Statistics*, pages 1022–1031, 2016.
- [22] Josip Djolonga, Andreas Krause, and Volkan Cevher. High-dimensional gaussian process bandits. In *Advances in Neural Information Processing Systems*, pages 1025–1033, 2013.
- [23] Ilija Bogunovic, Jonathan Scarlett, and Volkan Cevher. Time-varying gaussian process bandit optimization. In *Artificial Intelligence and Statistics*, pages 314–323, 2016.
- [24] Lihong Li, Wei Chu, John Langford, and Robert E Schapire. A contextual-bandit approach to personalized news article recommendation. In *Proceedings of the 19th international conference on World wide web*, pages 661–670. ACM, 2010.
- [25] Andreas Krause and Cheng S Ong. Contextual gaussian process bandit optimization. In *Advances in neural information processing systems*, pages 2447–2455, 2011.
- [26] Haitao Liu, Yew-Soon Ong, Xiaobo Shen, and Jianfei Cai. When gaussian process meets big data: A review of scalable gps. *arXiv preprint arXiv:1807.01065*, 2018.

Appendix A.

The SolveTwoLevelSparseLeastSquares Algorithm

The SOLVETWOLEVELSPARSELEASTSQUARES algorithm is listed in [2] and based on Theorem 2 of [2]. Given its centrality to Algorithm 2 we list it again here. The algorithm solves a sparse version of the the least squares problem:

$$\min_x \|\mathbf{b} - \mathbf{B}\mathbf{x}\|^2$$

which has solution $\mathbf{x} = \mathbf{A}^{-1}\mathbf{B}^T\mathbf{b}$ where $\mathbf{A} = \mathbf{B}^T\mathbf{B}$ and where \mathbf{B} and \mathbf{b} have the following structure:

$$\mathbf{B} \equiv \left[\begin{array}{c|c|c|c|c} \mathbf{B}_1 & \dot{\mathbf{B}}_1 & \mathbf{O} & \cdots & \mathbf{O} \\ \mathbf{B}_2 & \mathbf{O} & \dot{\mathbf{B}}_2 & \cdots & \mathbf{O} \\ \vdots & \vdots & \vdots & \ddots & \vdots \\ \mathbf{B}_m & \mathbf{O} & \mathbf{O} & \cdots & \dot{\mathbf{B}}_m \end{array} \right] \quad \text{and} \quad \mathbf{b} = \left[\begin{array}{c} \mathbf{b}_1 \\ \mathbf{b}_2 \\ \vdots \\ \mathbf{b}_m \end{array} \right]. \quad (12)$$

The sub-vectors of \mathbf{x} and the sub-matrices of \mathbf{A} corresponding to its non-zero blocks of are labelled as follows:

$$\mathbf{x} = \begin{bmatrix} \mathbf{x}_1 \\ \mathbf{x}_{2,1} \\ \mathbf{x}_{2,2} \\ \vdots \\ \mathbf{x}_{2,m} \end{bmatrix} \quad (13)$$

and

$$\mathbf{A}^{-1} = \begin{bmatrix} \mathbf{A}^{11} & \mathbf{A}^{12,1} & \mathbf{A}^{12,2} & \dots & \mathbf{A}^{12,m} \\ \mathbf{A}^{12,1T} & \mathbf{A}^{22,1} & \times & \dots & \times \\ \mathbf{A}^{12,2T} & \times & \mathbf{A}^{22,2} & \dots & \times \\ \vdots & \vdots & \vdots & \ddots & \vdots \\ \mathbf{A}^{12,mT} & \times & \times & \dots & \mathbf{A}^{22,m} \end{bmatrix} \quad (14)$$

with \times denoting sub-blocks that are not of interest. The SOLVETWOLEVELSPARSELEAST-SQUARES algorithm is given in Algorithm 4.

Algorithm 4 SOLVETWOLEVELSPARSELEASTSQUARES *for solving the two-level sparse matrix least squares problem: minimise $\|\mathbf{b} - \mathbf{B}\mathbf{x}\|^2$ in \mathbf{x} and sub-blocks of \mathbf{A}^{-1} corresponding to the non-zero sub-blocks of $\mathbf{A} = \mathbf{B}^T\mathbf{B}$. The sub-block notation is given by (12) and (14).*

Inputs: $\{(\mathbf{b}_i(\tilde{n}_i \times 1), \mathbf{B}_i(\tilde{n}_i \times p), \dot{\mathbf{B}}_i(\tilde{n}_i \times q)) : 1 \leq i \leq m\}$

$\omega_3 \leftarrow \text{NULL}$; $\Omega_4 \leftarrow \text{NULL}$

For $i = 1, \dots, m$:

Decompose $\dot{\mathbf{B}}_i = \mathbf{Q}_i \begin{bmatrix} \mathbf{R}_i \\ \mathbf{0} \end{bmatrix}$ such that $\mathbf{Q}_i^{-1} = \mathbf{Q}_i^T$ and \mathbf{R}_i is upper-triangular.

$\mathbf{c}_{0i} \leftarrow \mathbf{Q}_i^T \mathbf{b}_i$; $\mathbf{C}_{0i} \leftarrow \mathbf{Q}_i^T \mathbf{B}_i$; $\mathbf{c}_{1i} \leftarrow$ first q rows of \mathbf{c}_{0i}

$\mathbf{c}_{2i} \leftarrow$ remaining rows of \mathbf{c}_{0i} ; $\omega_3 \leftarrow \begin{bmatrix} \omega_3 \\ \mathbf{c}_{2i} \end{bmatrix}$

$\mathbf{C}_{1i} \leftarrow$ first q rows of \mathbf{C}_{0i} ; $\mathbf{C}_{2i} \leftarrow$ remaining rows of \mathbf{C}_{0i} ; $\Omega_4 \leftarrow \begin{bmatrix} \Omega_4 \\ \mathbf{C}_{2i} \end{bmatrix}$

Decompose $\Omega_4 = \mathbf{Q} \begin{bmatrix} \mathbf{R} \\ \mathbf{0} \end{bmatrix}$ such that $\mathbf{Q}^{-1} = \mathbf{Q}^T$ and \mathbf{R} is upper-triangular.

$\mathbf{c} \leftarrow$ first p rows of $\mathbf{Q}^T \omega_3$; $\mathbf{x}_1 \leftarrow \mathbf{R}^{-1} \mathbf{c}$; $\mathbf{A}^{11} \leftarrow \mathbf{R}^{-1} \mathbf{R}^{-T}$

For $i = 1, \dots, m$:

$\mathbf{x}_{2,i} \leftarrow \mathbf{R}_i^{-1}(\mathbf{c}_{1i} - \mathbf{C}_{1i} \mathbf{x}_1)$; $\mathbf{A}^{12,i} \leftarrow -\mathbf{A}^{11}(\mathbf{R}_i^{-1} \mathbf{C}_{1i})^T$

$\mathbf{A}^{22,i} \leftarrow \mathbf{R}_i^{-1}(\mathbf{R}_i^{-T} - \mathbf{C}_{1i} \mathbf{A}^{12,i})$

Output: $(\mathbf{x}_1, \mathbf{A}^{11}, \{(\mathbf{x}_{2,i}, \mathbf{A}^{22,i}, \mathbf{A}^{12,i}) : 1 \leq i \leq m\})$
